International Journal of Innovative
Computing, Information and Control
Volume **13**, Number **4**, August **2017**

ICIC International ©2017 ISSN 1349-4198
pp. 1273–1288

MIXED H_∞/PASSIVE PROJECTIVE SYNCHRONIZATION FOR FRACTIONAL-ORDER NEURAL NETWORKS WITH UNCERTAIN PARAMETERS AND DELAYS

Xiaona Song[1], Shuai Song[1] and Ines Tejado Balsera[2]

[1]School of Information Engineering
Henan University of Science and Technology
No. 263, Kaiyuan Ave., Luoyang 471023, P. R. China
{ xiaona_97; songshuai_1010 }@163.com

[2]Industrial Engineering School
University of Extremadura
Avenida de Elvas s/n, Badajoz 06006, Spain
itejbal@unex.es

Received December 2016; revised April 2017

Abstract. *This paper considers the design problem of mixed H_∞/passive projective synchronization for fractional-order (FO) neural networks with uncertain parameters and time-delays. Firstly, by use of active control and adaptive control method, efficient hybrid control strategies are designed for the synchronization of time-delayed FO dynamic networks with uncertain parameters. Then, a continuous frequency distributed model of the FO dynamic networks is given, via the application of FO system stability theory and robust control, the projective synchronization conditions are addressed in terms of linear matrix inequality techniques. Based on the conditions, a desired controller which can guarantee the robust stability of the closed-loop system and also ensure a mixed H_∞/passive performance level is designed. Finally, synchronization of two time-delayed FO dynamic networks with uncertain parameters and the application in secure communications as simulation examples are given to illustrate the effectiveness of the proposed method.*

Keywords: H_∞/passive performance, Adaptive projective synchronization, Fractional order neural networks, Time delay, Uncertain parameters

1. **Introduction.** The seeds of fractional derivatives were planted over 300 years ago, and fractional calculus is a field of applied mathematics that deals with derivatives and integrals of arbitrary orders (including complex orders). In recent years, it has played important roles in science, engineering, mathematics, economics, and other fields of pure and applied sciences because it allows modelling of real physical systems more accurately than calculus of integer order does [1,2]. When the model of a system includes at least one fraction derivative or integral term, we call it a fractional order system. One of the important applications of fractional calculus is in the area of fractional-order neural networks systems. The research related to fractional-order neural networks has received considerable attention, and some valuable results have been presented [3,4]. Due to the finite switching speed of amplifiers, time delay inevitably exists in neural networks. It can cause oscillation and instability behavior of systems [5]. Therefore, the study on stability analysis and controller design of fractional-order neural networks with time delays is of both theoretical and practical importance.

Since Pecora and Carroll [6] introduced a method to synchronize two identical chaotic systems with different initial conditions, synchronization has received considerable attention among scientists due to its importance in many applications such as secure communication, chemical systems, biological systems, and human heartbeat regulation. Since then, a variety of synchronization methods have been developed [7,8]. Furthermore, projective synchronization, characterized by a scaling factor that two systems synchronize proportionally, is one of the most interesting problems. Based on projective synchronization, sliding mode control was discussed in [9] for fractional order chaotic systems, and later, a modified projective synchronization for fractional order hyperchaotic systems was proposed in [10]. Function projective synchronization scheme was investigated in [11], and a modified function projective synchronization for a class of partial linear fractional-order chaotic system was studied in [12]. Very recently, some results with respect to projective synchronization of fractional-order neural networks have been proposed in [13,14].

On the other hand, the passivity theory plays an important role in the design and analysis of linear and nonlinear systems, which has attracted significant attention during the last decades. For fractional-order systems, passivity-based control approach was investigated in [15]. It is well realized that the purpose of H_∞ controllers/filters is to guarantee the closed-loop error systems are stable with an H_∞ norm bound limited to disturbance attenuation [16,17]. Recently, state feedback H_∞ control of commensurate fractional-order systems and H_∞ model reduction for positive fractional-order systems were investigated in [18,19], respectively. Noting the importance of H_∞ control theory and passivity theory, the mixed H_∞/passive performance index was first presented in [20]. Then, many authors have investigated the H_∞/passive control or synchronization for different systems, see, e.g., [21,22]. While for fractional-order neural networks, the projective synchronization problem based on the mixed H_∞/passive performance has been seldom studied which is one of our main motivations.

Motivated by the above discussions, our work is mainly to discuss the mixed H_∞/passive projective synchronization of fractional-order neural networks by using the adaptive control approach and in the presence of time-delay and model uncertainties. By combining the active control and adaptive control, a novel hybrid control scheme is designed, which is suitable for the time-delayed fractional-order neural networks with uncertain parameters. Then, by fractional-order Lyapunov theorem, stability analysis results are given in terms of linear matrix inequalities. Finally, numerical examples and the application in secure communications are presented to illustrate the effectiveness and validation of the proposed adaptive projective synchronization scheme.

2. Problem Formulation.

To discuss fractional-order systems, we often need to solve fractional-order differential equations. Some commonly used definitions and lemmas about fractional calculus are proposed.

Definition 2.1. [23] *The fractional integral of order α for a function f is defined as*

$$I^\alpha f(t) = \frac{1}{\Gamma(\alpha)} \int_{t_0}^{t} \frac{f(\tau)}{(t-\tau)^{1-\alpha}} d\tau \tag{1}$$

where $t \geq t_0$, $\alpha > 0$ and $\Gamma(\cdot)$ is the well-known gamma function.

Definition 2.2. [23] *The Caputo fractional derivative of order α of a function $f \in C^n([t_0, +\infty], R)$ is defined as*

$$D^\alpha f(t) = \begin{cases} \dfrac{1}{\Gamma(n-\alpha)} \int_{t_0}^{t} \dfrac{f^{(n)}(\tau)}{(t-\tau)^{\alpha+1-n}} d\tau, & n-1 < \alpha < n \\ \dfrac{d^n f(t)}{dt^n}, & \alpha = n \end{cases} \tag{2}$$

where $t \geq t_0$, n is the first integer which is not less than α, i.e., $n-1 \leq \alpha < n$. Particularly, when $0 < \alpha < 1$,

$$D^\alpha f(t) = \frac{1}{\Gamma(1-\alpha)} \int_{t_0}^{t} \frac{f'(\tau)}{(t-\tau)^\alpha} d\tau \tag{3}$$

Definition 2.3. [23] *Let $\Omega = [a, b]$ be an interval on the real axis R, let $n = [\alpha] + 1$ for $\alpha \notin N$ or $n = \alpha$ for $\alpha \in N$. If $y \in C^n[a, b]$, then*

$$I^\alpha D^\alpha y(t) = y(t) - \sum_{k=0}^{n-1} \frac{y^{(k)}(a)}{k!}(x-a)^k \tag{4}$$

In particular, if $0 < \alpha < 1$ and $y \in C^1[a, b]$, then

$$I^\alpha D^\alpha y(t) = y(t) - y(a) \tag{5}$$

Lemma 2.1. [24] *Let U, V, W and M be real matrices of appropriate dimensions with M satisfying $M = M^T$, then*

$$M + UVW + W^T V^T U^T < 0 \tag{6}$$

if and only if there exists a scalar $\varepsilon > 0$ such that

$$M + \varepsilon^{-1} U U^T + \varepsilon W^T W < 0 \tag{7}$$

In this section, we consider the time-delayed fractional-order neural networks as the drive system, which can be described by the following differential equation:

$$D^\alpha x(t) = -Cx(t) + (A + \Delta A) f(x(t)) + (B + \Delta B) f(x(t - \tau_1)) + H_1 \omega(t) \tag{8}$$

$$z(t) = Jx(t) \tag{9}$$

where $x(t) = [x_1(t), x_2(t), \ldots, x_n(t)]^T \in R^n$ is the state vector of the neural network system (8) and (9). $z(t)$ is the output, $C = diag(c_1, c_2, \ldots, c_n)$ represents the self-connection weight, where c_i $(i = 1, 2, \ldots, n) \in R$, $A = (a_{ij})_{n \times n}$, $B = (b_{kj})_{n \times n}$ are the interconnection weight matrix, $H_1 \in R^{n \times n}$ is a known real constant matrix and τ_1 stands for a time delay, which is a positive constant, and $f(x(t)) = [f_1(x_1(t)), f_2(x_2(t)), \ldots, f_n(x_n(t))]^T \in R^n$ represents the activation function and $\omega(t) = [\omega_1(t), \omega_2(t), \ldots, \omega_n(t)]^T$ denotes the disturbance input that belongs to $L_2[0, \infty)$. The parameter uncertainties ΔA_i, ΔB_i are time varying matrices with appropriate dimensions, which are defined as follows

$$[\Delta A, \Delta B] = DF(t)[E_1, E_2] \tag{10}$$

where D, E_1, E_2 are known constant matrices of appropriate dimensions and $F(t)$ is a known time varying matrix with Lebegue measurable elements bounded by

$$F^T(t) F(t) \leq I \tag{11}$$

where I is the identity matrix with appropriate dimension.

The response system is described by

$$D^\alpha y(t) = -Cy(t) + (A + \Delta A) f(y(t)) + (B + \Delta B) f(y(t - \tau_2)) + H_2 \omega(t) + u(t) \tag{12}$$

$$\tilde{z}(t) = Jy(t) \tag{13}$$

where $y(t) = [y_1(t), y_2(t), \dots, y_n(t)]^T \in R^n$ is the state vector of the response system (12) and (13), $\tilde{z}(t)$ is the output, $u(t) = [u_1(t), u_2(t), \dots, u_n(t)]^T \in R^n$ is a control input vector and $H_2 \in R^{n\times n}$ is a known real constant matrix with appropriate dimensions.

Assumption 2.1. [25] *The neuron activation function f_i is bounded and satisfies Lipschitz condition on R, that is, there exists constant $l_i > 0$ such that*

$$|f_i(\phi) - f_i(\varphi)| \le l_i \, |\phi - \varphi| \tag{14}$$

for any $\phi, \varphi \in R$. For convenience, we define $L = diag(l_1, l_2, \dots, l_n)$.

Definition 2.4. *The systems (8) and (12) can achieve projective synchronization if there exists a nonzero constant β and controller $u_i(t)$ $(i = 1, 2, \dots, n)$ for any two solutions $x(t)$ and $y(t)$ of systems (8) and (12) with different initial values $x(0)$ and $y(0)$ such that*

$$\lim_{t\to\infty} \|y(t) - \beta x(t)\| = 0 \tag{15}$$

Our objective is to find suitable and effective controller functions $u_i(t)$ $(i = 1, 2, \dots, n)$ to ensure the asymptotically stability of the error system and satisfy the mixed H_∞/passive performance, which is defined in the following.

Definition 2.5. *Given a weight scalar $\sigma \in (0, 1)$, the synchronization error system between systems (8) and (12): $e(t) = y(t) - \beta x(t)$ is said to be asymptotically stable and satisfy a mixed H_∞/passive performance δ, if the following two requirements are satisfied simultaneously:*

(1) the synchronization error system between systems (8) and (12) is asymptotically stable;

(2) under zero initial condition, there exists a scalar $\delta > 0$ such that the following condition is satisfied:

$$\int_0^{T_p} \left[-\sigma \hat{z}^T(t)\hat{z}(t) + 2(1-\sigma)\delta \hat{z}^T(t)\omega(t)\right] dt \ge -\delta^2 \int_0^{T_p} \left[\omega^T(t)\omega(t)\right] dt \tag{16}$$

for any $T_p > 0$ and any non-zero $\omega(t) \in L_2[0, \infty)$, where $\hat{z}(t) = Je(t)$.

Remark 2.1. *It has been recognized that the time-delays and parameter uncertainties, which are inherent features of many physical processes, are very often the cause for instability and poor performance of systems. As for the fractional-order complex networks with parametric uncertainties, the issue of synchronization has been well investigated in [26]. Also, the synchronization problem for time-delay fractional-order neural networks has been tackled in [27,28], respectively. Unfortunately, the parametric uncertainties and the time delays have not been considered in [26-28] simultaneously for the synchronization problem of fractional-order neural networks. Especially, our proposed synchronization controller not only can guarantee the robust stability of the closed-loop system, but also ensures a mixed H_∞/passive performance level.*

3. **Synchronization Controller Design and Analysis.** Firstly, we define synchronization error as follows

$$e(t) = y(t) - \beta x(t) \tag{17}$$

Then based on Definition 2.3, the error dynamical system can be obtained as follows

$$\begin{aligned} D^\alpha e(t) = & -Ce(t) + (A + \Delta A)[f(y(t)) - \beta f(x(t))] \\ & + (B + \Delta B)\left[f(y(t-\tau_2)) - \beta f(x(t-\tau_1))\right] + (H_2 - \beta H_1)\omega(t) + u(t) \end{aligned} \tag{18}$$

where $e(t) = [e_1(t), e_2(t), \dots, e_n(t)]^T \in R^n$ are state vectors of error system (18), $\beta = diag[\beta_1(t), \beta_2(t), \beta_3(t)]$ is continuous vector function.

Remark 3.1. *If $\beta_1 = \beta_2 = \beta_3 = 1$ or $\beta_1 = \beta_2 = \beta_3 = -1$, the proposed projective synchronization problem will be reduced to the common synchronization or anti-synchronization. If $\beta_1 = \beta_2 = \beta_3 = 0$, the projective synchronization problem will be turned to a stabilization problem of fractional-order delayed neural network system.*

Remark 3.2. *If $\beta_1 \neq \beta_2 \neq \beta_3$ are time-varying parameters, the proposed projective synchronization problem is said to be function projective synchronization of fractional-order dynamic networks.*

In what follows, we will design appropriate control scheme to ensure the projective synchronization can be achieved between the drive system (8) and the response system (12).

At first, the control input $u(t)$ is designed as the following:

$$u(t) = v(t) + w(t) \tag{19}$$

where

$$v(t) = (A + \Delta A)[\beta f(x(t)) - f(\beta x(t))] + (B + \Delta B)[\beta f(x(t-\tau_1)) - f(\beta x(t-\tau_2))],$$
$$w(t) = -K(t)e(t),$$
$$K(t) = diag(k_1(t), k_2(t), \dots, k_n(t)),$$

and

$$\dot{k}_i(t) = \sum_{j=1}^{n} e_j(t)\left[2\lambda_i P_{1ji} + 2\lambda_i P_{2ji} + \lambda_i P_{3ji}\right] e_i(t) + \sum_{j=1}^{n} D^\alpha e_j(t) P_{3ji} \lambda_i D^\alpha e_i(t) \tag{20}$$

where λ_i $(i = 1, 2, \dots, n)$ are positive constants.

Now, by applying the control scheme (19) to the error system (18), the following error dynamic can be obtained

$$\begin{aligned} D^\alpha e(t) = & -Ce(t) + (A + \Delta A)\left[f(y(t)) - f(\beta x(t))\right] \\ & + (B + \Delta B)\left[f(y(t-\tau_2)) - f(\beta x(t-\tau_2))\right] \\ & + (H_2 - \beta H_1)\omega(t) - K(t)e(t) \end{aligned} \tag{21}$$

Based on Equation (10), the error system (21) can be rewritten as

$$\begin{aligned} D^\alpha e(t) = & -Ce(t) + (A + DF(t)E_1)[f(y(t)) - f(\beta x(t))] \\ & + (B + DF(t)E_2)[f(y(t-\tau_2)) - f(\beta x(t-\tau_2))] \\ & + (H_2 - \beta H_1)\omega(t) - K(t)e(t) \end{aligned} \tag{22}$$

$$\hat{z}(t) = Je(t) \tag{23}$$

It is obvious that $e(t) = 0$ is a trivial solution of the error system (22).

Based on a continuous frequency distributed model of Caputo derivatives proposed in [29], the error system (22) can be expressed as

$$\begin{cases} \dfrac{\partial Z(\omega,t)}{\partial t} = -\omega Z(\omega,t) - Ce(t) + (A + \Delta A)[f(y(t)) - f(\beta x(t))] \\ \qquad\qquad +(B + \Delta B)[f(y(t-\tau_2)) - f(\beta x(t-\tau_2))] \\ \qquad\qquad +(H_2 - \beta H_1)\omega(t) - K(t)e(t) \\ e(t) = \int_0^\infty \mu(\omega) Z(\omega,t) d\omega \end{cases} \tag{24}$$

where $Z(\omega,t) = [Z_1(\omega,t), Z_2(\omega,t), \dots, Z_n(\omega,t)]^T$, $\mu(\omega) = \mathrm{diag}\,[\mu_1(\omega), \mu_2(\omega), \dots, \mu_n(\omega)]$ and $\mu_i(\omega) = \frac{\sin(p\pi)}{\pi}\omega^{-p}$.

Next, we mainly prove the stability of the error system (22) for the zero solution.

Theorem 3.1. *Let Assumption 2.1 be satisfied, for given scalars α, β, δ, γ and $0 < \sigma < 1$, matrix J and adaptive constant matrix K, if there exist positive definite matrices P_1, P_2, P_3, R and ε_i $(i = 1, 2, \dots, 6)$, such that*

$$\begin{bmatrix} \Omega_1 & \Omega_2 & \Omega_3 & \Omega_4 \\ * & -R_1 & 0 & 0 \\ * & * & -R_2 & 0 \\ * & * & * & -R_3 \end{bmatrix} < 0 \tag{25}$$

where

$$\Omega_1 = \begin{bmatrix} \psi_{11} & \psi_{12} & \psi_{13} & \hat{\varphi}_{14} \\ * & \psi_{22} & \psi_{23} & \hat{\varphi}_{24} \\ * & * & \hat{\varphi}_{33} & \hat{\varphi}_{34} \\ * & * & * & \hat{\varphi}_{44} \end{bmatrix}, \quad \Omega_2 = \begin{bmatrix} P_1D & L_1^TE_1^T\varepsilon_1 & P_1D & L_2^TE_2^T\varepsilon_2 \\ 0 & 0 & 0 & 0 \\ 0 & 0 & 0 & 0 \\ 0 & 0 & 0 & 0 \end{bmatrix},$$

$$\Omega_3 = \begin{bmatrix} P_2D & L_1^TE_1^T\varepsilon_3 & P_2D & L_2^TE_2^T\varepsilon_4 \\ 0 & 0 & 0 & 0 \\ 0 & 0 & 0 & 0 \\ 0 & 0 & 0 & 0 \end{bmatrix},$$

$$\Omega_4 = \begin{bmatrix} P_3D & L_1^TE_1^T\varepsilon_5 & 0 & 0 & 0 & 0 \\ 0 & 0 & P_1D & L_2^TE_2^T\varepsilon_2 & P_3D & L_2^TE_2^T\varepsilon_6 \\ 0 & 0 & 0 & 0 & 0 & 0 \\ 0 & 0 & 0 & 0 & 0 & 0 \end{bmatrix},$$

$$R_1 = diag\{\varepsilon_1I, \varepsilon_1I, \varepsilon_2I, 2\varepsilon_2I\}, \quad R_2 = diag\{2\varepsilon_3I, \varepsilon_3I, \varepsilon_4I, \varepsilon_4I\},$$
$$R_3 = diag\{2\varepsilon_5I, 2\varepsilon_5I, 2\varepsilon_2I, 2\varepsilon_2I, 2\varepsilon_6I, 2\varepsilon_6I\},$$

and

$$\begin{aligned}
\psi_{11} = & -P_1C - C^TP_1 + P_1AL_1 + L_1^TA^TP_1 - P_1K - K^TP_1 + \frac{1}{2}P_1BL_2 + \frac{1}{2}L_2^TB^TP_1 \\
& - P_2K - K^TP_2 - P_2C - C^TP_2 + P_2AL_1 + L_1^TA^TP_2 + \sigma J^TJ, \\
\psi_{12} = & P_2BL_2 + L_2^TB^TP_2, \quad \psi_{13} = -P_2 - C^TP_3 + \frac{1}{2}P_3AL_1 + \frac{1}{2}L_1^TA^TP_3, \\
\hat{\varphi}_{14} = & P_1H_2 - \beta P_1H_1 + P_2H_2 - \beta P_2H_1 - (1-\sigma)\delta J^T, \\
\psi_{22} = & \frac{1}{2}P_1BL_2 + \frac{1}{2}L_2^TB^TP, \quad \psi_{23} = \frac{1}{2}P_3BL_2 + \frac{1}{2}L_2^TB^TP_3, \\
\hat{\varphi}_{24} = & 0, \quad \hat{\varphi}_{33} = -2P_3, \quad \hat{\varphi}_{34} = P_3H_2 - \beta P_3H_1, \quad \hat{\varphi}_{44} = R - \delta^2I,
\end{aligned}$$

then the synchronization error system between systems (8) and (12) is asymptotically stable with a prescribed mixed H_∞/passive performance level δ.

Proof: Considering the following Lyapunov functional for systems (22) and (23)

$$V(t) = V_1(t) + V_2(t) + V_3(t) \tag{26}$$

where

$$V_1(t) = \int_0^\infty Z^T(\omega, t)\mu(\omega)P_1Z(\omega, t)d\omega,$$
$$V_2(t) = \sum_{i=1}^n \frac{1}{2\lambda_i}(k_i(t) - k_i)^2, \quad V_3(t) = \int_0^t \omega^T(s)R\omega(s)ds.$$

Taking the time fractional-order derivative of $V(t)$ and combining Equations (24), (10) and (20) give the following result:

$$\begin{aligned}\dot{V}(t) = & \int_0^\infty [-\omega Z(\omega,t) - Ce(t) + (A + DF(t)E_1)\psi(e(t)) \\ & + (B + DF(t)E_2)\psi(e(t-\tau_2)) - K(t)e(t) + (H_2 - \beta H_1)\omega(t)]^T \mu(\omega) P_1 Z(\omega,t) d\omega \\ & + \int_0^\infty Z^T(\omega,t)\mu(\omega)P_1[-\omega Z(\omega,t) - Ce(t) + (A + DF(t)E_1)\psi(e(t)) \\ & + (B + DF(t)E_2)\psi(e(t-\tau_2)) - K(t)e(t) + (H_2 - \beta H_1)\omega(t)]d\omega \\ & + \sum_{i=1}^n \frac{1}{\lambda_i}(k_i(t) - k_i)\left[2\sum_{i=1}^n e_j(t)P_{1ji}\lambda_i e_i(t) + 2\sum_{i=1}^n e_j(t)P_{2ji}\lambda_i e_i(t)\right. \\ & \left. + \sum_{i=1}^n e_j(t)P_{3ji}\lambda_i e_i(t) + \sum_{i=1}^n D^\alpha e_j(t)P_{3ji}\lambda_i D^\alpha e_i(t)\right] + \omega^T(t)R\omega(t),\end{aligned}$$

where $\psi(e(t)) = f(y(t)) - f(\beta x(t))$, $\psi(e(t-\tau_2)) = f(y(t-\tau_2)) - f(\beta x(t-\tau_2))$.

Now, based on Assumption 2.1, we have

$$\begin{aligned}\dot{V}(t) \leq & \int_0^\infty [-\omega Z(\omega,t) - Ce(t) + (A + DF(t)E_1)L_1 e(t) \\ & + (B + DF(t)E_2)L_2 e(t-\tau_2) \\ & + (H_2 - \beta H_1)\omega(t) - K(t)e(t)]^T \mu(\omega)P_1 Z(\omega,t)d\omega \\ & + \int_0^\infty Z^T(\omega,t)\mu(\omega)P_1[-\omega Z(\omega,t) - Ce(t) + (A + DF(t)E_1)L_1 e(t) \\ & + (B + DF(t)E_2)L_2 e(t-\tau_2) + (H_2 - \beta H_1)\omega(t) - K(t)e(t)]d\omega \\ & + \sum_{i=1}^n \frac{1}{\lambda_i}(k_i(t) - k_i)\left[2\sum_{i=1}^n e_j(t)P_{1ji}\lambda_i e_i(t) + 2\sum_{i=1}^n e_j(t)P_{2ji}\lambda_i e_i(t)\right. \\ & \left. + \sum_{i=1}^n e_j(t)P_{3ji}\lambda_i e_i(t) + \sum_{i=1}^n D^\alpha e_j(t)P_{3ji}\lambda_i D^\alpha e_i(t)\right] + \omega^T(t)R\omega(t)\end{aligned} \tag{27}$$

From Equation (24), (27) can be rewritten as follows:

$$\begin{aligned}\dot{V}(t) \leq & e^T(t)\left[-P_1 C - C^T P_1 + P_1 A L_1 + L_1^T A^T P_1 + P_1 DF(t)E_1 L_1 + L_1^T E_1^T F^T(t) D^T P_1\right. \\ & \left. - P_1 K - K^T P_1\right] e(t) + 2e^T(t)\left[P_1 B L_2 + P_1 DF(t) E_2 L_2\right] e(t-\tau_2) \\ & + 2e^T(t)[P_1 H_2 - \beta P_1 H]\omega(t) + 2e^T(t)P_2(K(t) - K)e(t) \\ & + (D^\alpha e(t))^T P_3(K(t) - K)D^\alpha e(t) + \omega^T(t)R\omega(t) \\ \leq & e^T(t)\Big[-P_1 C - C^T P_1 + P_1 A L_1 + L_1^T A^T P_1 + P_1 DF(t)E_1 L_1 + L_1^T E_1^T F^T(t) D^T P_1 \\ & - P_1 K - K^T P_1 + \frac{1}{2}P_1 B L_2 + \frac{1}{2}L_2^T B^T P_1 + \frac{1}{2}P_1 DF(t)E_2 L_2 \\ & + \frac{1}{2}L_2^T E_2^T F^T(t) D^T P_1 + 2P_2(K(t) - K)\Big] e(t) \\ & + e^T(t-\tau_2)\Big[\frac{1}{2}P_1 B L_2 + \frac{1}{2}L_2^T B^T P + \frac{1}{2}P_1 DF(t)E_2 L_2\end{aligned}$$

$$+ \frac{1}{2}L_2^T E_2^T F^T(t) D^T P_1\Big] e(t-\tau_2) + 2e^T(t)[P_1 H_2 - \beta P_1 H]\omega(t)$$
$$+ (D^\alpha e(t))^T P_3 (K(t) - K) D^\alpha e(t) + \omega^T(t) R \omega(t).$$

from which we get

$$\dot{V}(t) \le \eta^T(t) \begin{bmatrix} \varphi_{11} & \varphi_{12} & \varphi_{13} & \varphi_{14} \\ * & \varphi_{22} & \varphi_{23} & \varphi_{24} \\ * & * & \varphi_{33} & \varphi_{34} \\ * & * & * & \varphi_{44} \end{bmatrix} \eta(t) \tag{28}$$

where

$$\eta^T(t) = \left[\begin{array}{cccc} e^T(t) & e^T(t-\tau_2) & D^{\alpha^T} e(t) & \omega^T(t) \end{array}\right],$$

and

$$\begin{aligned} \varphi_{11} = &\ - P_1 C - C^T P_1 + P_1 A L_1 + L_1^T A^T P_1 + P_1 D F(t) E_1 L_1 + L_1^T E_1^T F^T(t) D P_1 \\ &- P_1 K - K^T P_1 + \frac{1}{2} P_1 B L_2 + \frac{1}{2} L_2^T B^T P_1 + \frac{1}{2} P_1 D F(t) E_2 L_2 \\ &+ \frac{1}{2} L_2^T E_2^T F^T(t) D P_1 + 2P_2(K(t) - K), \\ \varphi_{12} = &\ \varphi_{13} = \varphi_{23} = \varphi_{24} = \varphi_{34} = 0, \quad \varphi_{14} = P_1 H_2 - \beta P_1 H_1, \\ \varphi_{22} = &\ \frac{1}{2} P_1 B L_2 + \frac{1}{2} L_2^T B^T P + \frac{1}{2} P_1 D F(t) E_2 L_2 + + \frac{1}{2} L_2^T E_2^T F^T(t) D P, \\ \varphi_{33} = &\ P_3(K(t) - K), \quad \varphi_{44} = R. \end{aligned}$$

Then, from Equation (22), it is easy to see that for any appropriately dimensioned matrices P_2 and P_3, the following equation holds:

$$\begin{aligned} 0 = 2\left[e^T(t) P_2 + D^{\alpha^T} e(t) P_3\right] \{&-D^\alpha e(t) - C e(t) + (A + DF(t)E_1)\varphi(e(t)) \\ &+ (B + DF(t)E_2)\varphi(e(t-\tau_2)) + (H_2 - \beta H_1)\omega(t) - K(t) e(t)\} \end{aligned} \tag{29}$$

Adding the right-hand sides of (29) to $\dot{V}(t)$, we can get from (28)

$$\begin{aligned} &\dot{V}(t) + \sigma \hat{z}^T(t) \hat{z}(t) - 2(1-\sigma)\delta \hat{z}^T(t) \omega(t) - \delta^2 \omega^T(t) \omega(t) \\ &\le \eta^T(t) \begin{bmatrix} \tilde{\varphi}_{11} & \tilde{\varphi}_{12} & \tilde{\varphi}_{13} & \tilde{\varphi}_{14} \\ * & \tilde{\varphi}_{22} & \tilde{\varphi}_{23} & \tilde{\varphi}_{24} \\ * & * & \tilde{\varphi}_{33} & \tilde{\varphi}_{34} \\ * & * & * & \tilde{\varphi}_{44} \end{bmatrix} \eta(t), \end{aligned}$$

where

$$\begin{aligned} \tilde{\varphi}_{11} = &\ - P_1 C - C^T P_1 + P_1 A L_1 + L_1^T A^T P_1 + P_1 D F(t) E_1 L_1 + L_1^T E_1^T F^T(t) D^T P_1 \\ &- P_1 K - K^T P_1 + \frac{1}{2} P_1 B L_2 + \frac{1}{2} L_2^T B^T P_1 + \frac{1}{2} P_1 D F(t) E_2 L_2 \\ &+ \frac{1}{2} L_2^T E_2^T F^T(t) D^T P_1 - P_2 K - K^T P_2 - P_2 C - C^T P_2 + P_2 A L_1 + L_1^T A^T P_2 \\ &+ P_2 D F(t) E_1 L_1 + L_1^T E_1^T F^T(t) D^T P_2 - \frac{1}{2} P_3 K - \frac{1}{2} K^T P_3 + \sigma J^T J, \end{aligned}$$

$$\tilde{\varphi}_{12} = P_2BL_2 + L_2^TB^TP_2 + P_2DF(t)E_2L_2 + L_2^TE_2^TF^T(t)D^TP_2,$$
$$\tilde{\varphi}_{13} = -P_2 - C^TP_3 + \frac{1}{2}P_3AL_1 + \frac{1}{2}L_1^TA^TP_3 + \frac{1}{2}P_3DF(t)E_1L_1 + \frac{1}{2}L_1^TE_1^TF^T(t)D^TP_3,$$
$$\tilde{\varphi}_{14} = P_1H_2 - \beta P_1H_1 + P_2H_2 - \beta P_2H_1 - (1-\sigma)\delta J^T,$$
$$\tilde{\varphi}_{22} = \frac{1}{2}P_1BL_2 + \frac{1}{2}L_2^TB^TP + \frac{1}{2}P_1DF(t)E_2L_2 + +\frac{1}{2}L_2^TE_2^TF^T(t)D^TP_1,$$
$$\tilde{\varphi}_{23} = \frac{1}{2}P_3BL_2 + \frac{1}{2}L_2^TB^TP_3 + \frac{1}{2}P_3DF(t)E_2L_2 + \frac{1}{2}L_2^TE_2^TF^T(t)D^TP_3,$$
$$\tilde{\varphi}_{24} = 0,\ \tilde{\varphi}_{33} = -2P_3 - P_3K,\ \tilde{\varphi}_{34} = P_3H_2 - \beta P_3H_1,\ \tilde{\varphi}_{44} = R - \delta^2 I.$$

Based on Lemma 2.1, the above inequality can be rewritten as

$$\dot{V}(t) + \sigma\hat{z}^T(t)\hat{z}(t) - 2(1-\sigma)\delta\hat{z}^T(t)\omega(t) - \delta^2\omega^T(t)\omega(t)$$
$$\leq \eta^T(t)\begin{bmatrix} \hat{\varphi}_{11} & \hat{\varphi}_{12} & \hat{\varphi}_{13} & \hat{\varphi}_{14} \\ * & \hat{\varphi}_{22} & \hat{\varphi}_{23} & \hat{\varphi}_{24} \\ * & * & \hat{\varphi}_{33} & \hat{\varphi}_{34} \\ * & * & * & \hat{\varphi}_{44} \end{bmatrix}\eta(t),$$

with

$$\begin{aligned}\hat{\varphi}_{11} = & -P_1C - C^TP_1 + P_1AL_1 + L_1^TA^TP_1 + \varepsilon_1^{-1}P_1DD^TP_1 + \varepsilon_1L_1^TE_1^TE_1L_1 \\ & - P_1K - K^TP_1 + \frac{1}{2}P_1BL_2 + \frac{1}{2}L_2^TB^TP_1 + \frac{1}{2}\varepsilon_2^{-1}P_1DD^TP_1 \\ & + \frac{1}{2}\varepsilon_2L_2^TE_2^TE_2L_2 - P_2K - K^TP_2 - P_2C - C^TP_2 + P_2AL_1 + L_1^TA^TP_2 \\ & + \varepsilon_3^{-1}P_2DD^TP_2 + \varepsilon_3L_1^TE_1^TE_1L_1 + \sigma J^TJ,\end{aligned}$$
$$\hat{\varphi}_{12} = P_2BL_2 + L_2^TB^TP_2 + \varepsilon_4^{-1}P_2DD^TP_2 + \varepsilon_4L_2^TE_2^TE_2L_2,$$
$$\hat{\varphi}_{13} = -P_2 - C^TP_3 + \frac{1}{2}P_3AL_1 + \frac{1}{2}L_1^TA^TP_3 + \frac{1}{2}\varepsilon_5^{-1}P_3DD^TP_3 + \frac{1}{2}\varepsilon_5L_1^TE_1^TE_1L_1,$$
$$\hat{\varphi}_{22} = \frac{1}{2}P_1BL_2 + \frac{1}{2}L_2^TB^TP + \frac{1}{2}\varepsilon_2^{-1}P_1DD^TP_1 + \frac{1}{2}\varepsilon_2L_2^TE_2^TE_2L_2,$$
$$\hat{\varphi}_{23} = \frac{1}{2}P_3BL_2 + \frac{1}{2}L_2^TB^TP_3 + \frac{1}{2}\varepsilon_6^{-1}P_3DD^TP_3 + +\frac{1}{2}\varepsilon_6L_2^TE_2^TE_2L_2,$$

and the other parameters are the same in (25). Then, using Schur complement and pre-multiplying and post-multiplying the obtained inequality by

$$diag(I, I, I, I, I, \varepsilon_1I, I, \varepsilon_2I, I, \varepsilon_3I, I, \varepsilon_4I, I, \varepsilon_5I, I, \varepsilon_2I, I, \varepsilon_6I).$$

then we can obtain (25). This completes the proof.

4. **Numerical Simulation.** In this section, we give two simulation examples to illustrate the effectiveness of the proposed method and controllers for delayed fractional-order neural network system with parameter uncertainties. Firstly, initial values are selected as follows:

$$\alpha = 0.995, \quad \tau_1 = 0.001, \quad \tau_2 = 0.005, \quad \lambda_1 = \lambda_2 = \lambda_3 = 5,$$
$$A = \begin{bmatrix} 2 & -1.2 & 0 \\ 1.8 & 1.71 & 1.15 \\ -4.75 & 0 & 1.1 \end{bmatrix}, \quad B = \begin{bmatrix} -0.2 & 0.3 & 0 \\ -0.2 & -0.19 & -0.15 \\ 0.6 & 0 & -0.2 \end{bmatrix},$$
$$C = diag(1,1,1), \quad L_1 = L_2 = diag(1,1,1), \quad K = diag(2,2,2),$$
$$E_1 = E_2 = diag(0.02, 0.02, 0.02), \quad D = diag(0.01, 0.01, 0.01),$$
$$F(t) = 0.1\sin(t), \quad k_1(0) = 0.05, \quad k_2(0) = 0.06, \quad k_3(0) = 0.08.$$

Example 1:

Case 1: $\beta_1 = \beta_2 = \beta_3$ are selected as constants, e.g., $\beta_1 = \beta_2 = \beta_3 = 3$, and

$$x_1(0) = 0.1, \quad x_2(0) = 0.4, \quad x_3(0) = 0.2,$$
$$y_1(0) = 0.8, \quad y_2(0) = 0.1, \quad y_3(0) = 0.7.$$

After using an appropriate LMI solver to get the feasible numerical solution based on inequality (25), we can obtain that the positive definite matrices P_1, P_2, P_3 and variables ε_1, ε_2, ε_3 could be

$$P_1 = \begin{bmatrix} 1.6671 & 0.5568 & 0.6284 \\ 0.5568 & 0.7896 & 0.0434 \\ 0.6284 & 0.0434 & 0.6562 \end{bmatrix}, \quad P_2 = \begin{bmatrix} 0.1570 & -0.0482 & -0.0046 \\ -0.0482 & 0.1302 & 0.0520 \\ -0.0046 & 0.0520 & 0.1843 \end{bmatrix},$$

$$P_3 = \begin{bmatrix} 1.8640 & -0.8946 & -0.6145 \\ -0.8946 & 1.8304 & 0.8505 \\ -0.6145 & 0.8505 & 0.8652 \end{bmatrix}, \quad \begin{matrix} \varepsilon_1 = 42.5351, & \varepsilon_2 = 20.4439, & \varepsilon_3 = 42.5349, \\ \varepsilon_4 = 42.5349, & \varepsilon_5 = 21.7231, & \varepsilon_6 = 19.2881. \end{matrix}$$

The simulation results are shown in Figures 1-4. Figures 1-3 display the uncontrolled state trajectories $\beta_i x_i(t)$, $y_i(t)$ $(i = 1, 2, 3)$ between drive system and response system. In Figure 4, the state trajectories of error system asymptotically converge to zero by using the proposed control scheme, which implies that the projective synchronization can be achieved for systems (8) and (12).

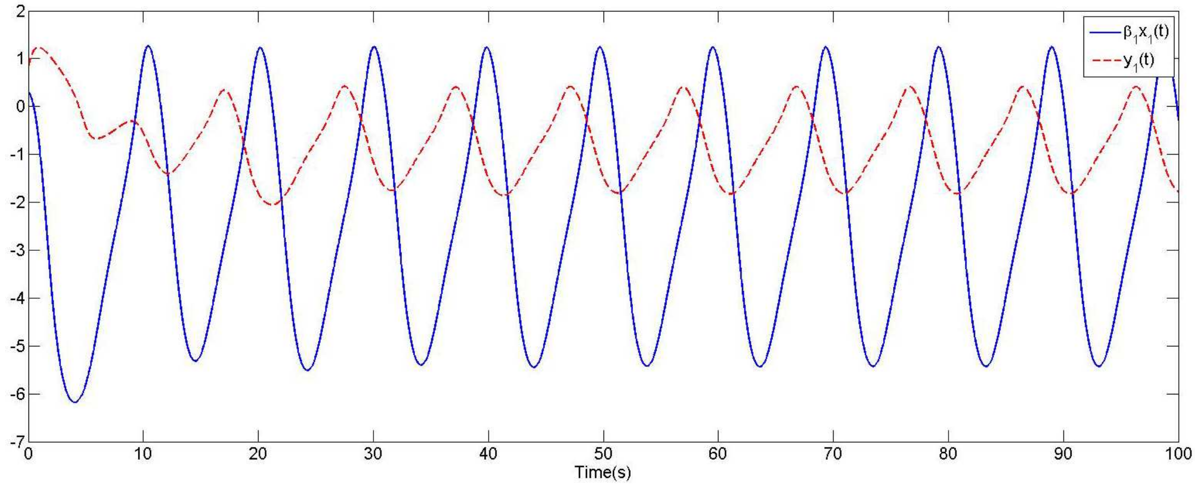

FIGURE 1. The uncontrolled state trajectories $\beta_1 x_1(t)$, $y_1(t)$ of the systems (8) and (12)

Case 2: The application of fractional-order neural network system synchronization in secure communication is investigated. The sketch designed for the communication scheme using our proposed synchronization method is similar to Figure 5 in [30].

In the transmitter, the original information signal $S(t)$ is modulated into the chaotic signal by using an invertible function Φ, i.e., $S'(t) = \Phi(x_1, x_2, x_3, S(t))$. Then we add the signal $S'(t)$ to one of the three variables x_1, x_2, x_3. For instance, we inject the signal $S'(t)$ into the variable x_1 and derive a combined signal $\chi(t) = x_1 + S'(t)$. In the channel, the variables x_1, x_2, x_3 and combined signal are transmitted to receiver. When the synchronization of master-slave system was achieved, the state y_1 will tend to βx_1; thus $S'(t)$ can be derived through a simple transformation $S'(t) = \chi(t) - {}^{y_1}\!/_{\beta}$. Further, the information signal can be recovered.

Here, we firstly choose an impulse signal, which is shown in Figure 5 as the information signal. The function Φ is given by $S'(t) = x_1 + S(t)$. We assume that the signal $S'(t)$ is

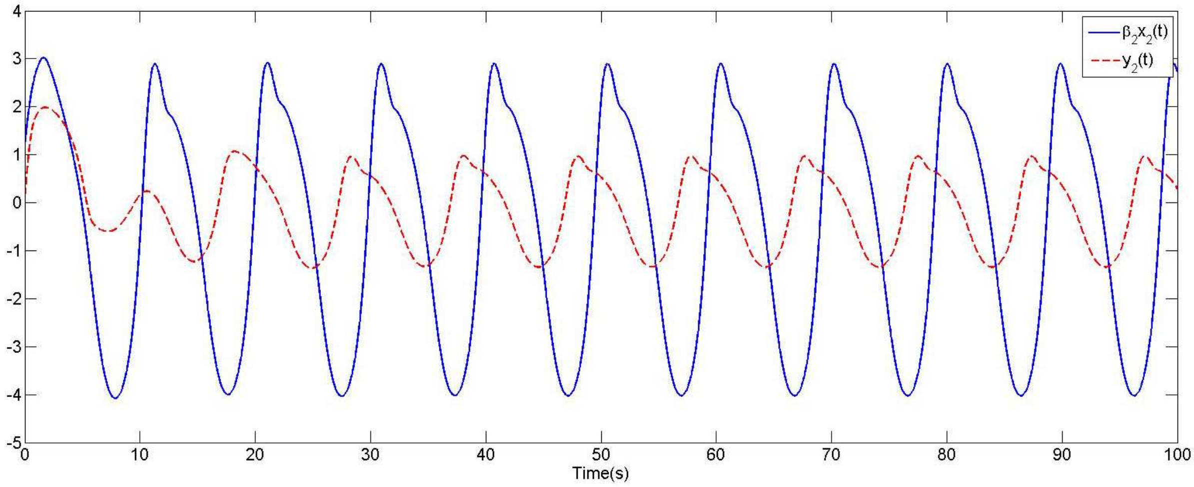

FIGURE 2. The uncontrolled state trajectories $\beta_2 x_2(t)$, $y_2(t)$ of the systems (8) and (12)

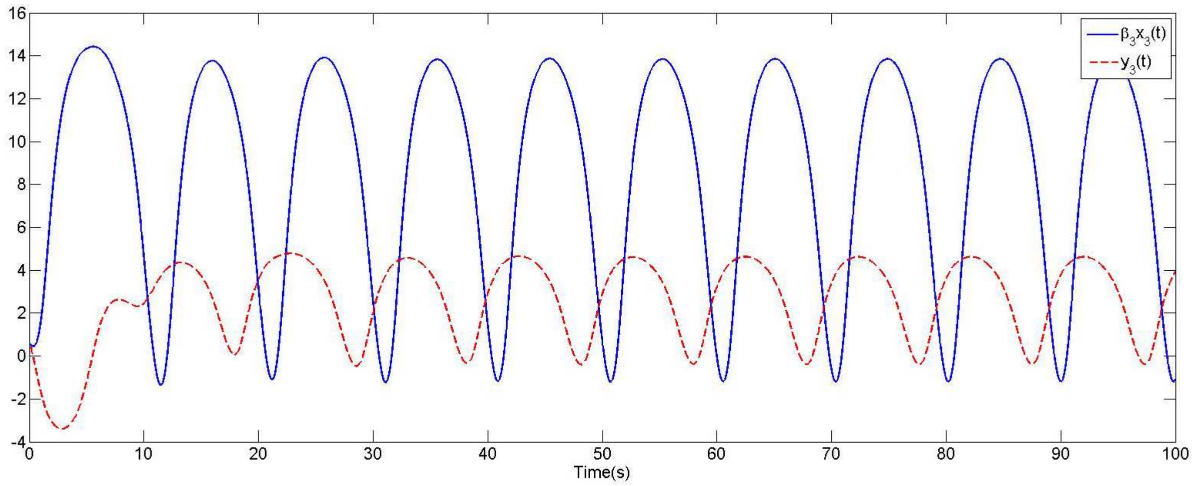

FIGURE 3. The uncontrolled state trajectories $\beta_3 x_3(t)$, $y_3(t)$ of the systems (8) and (12)

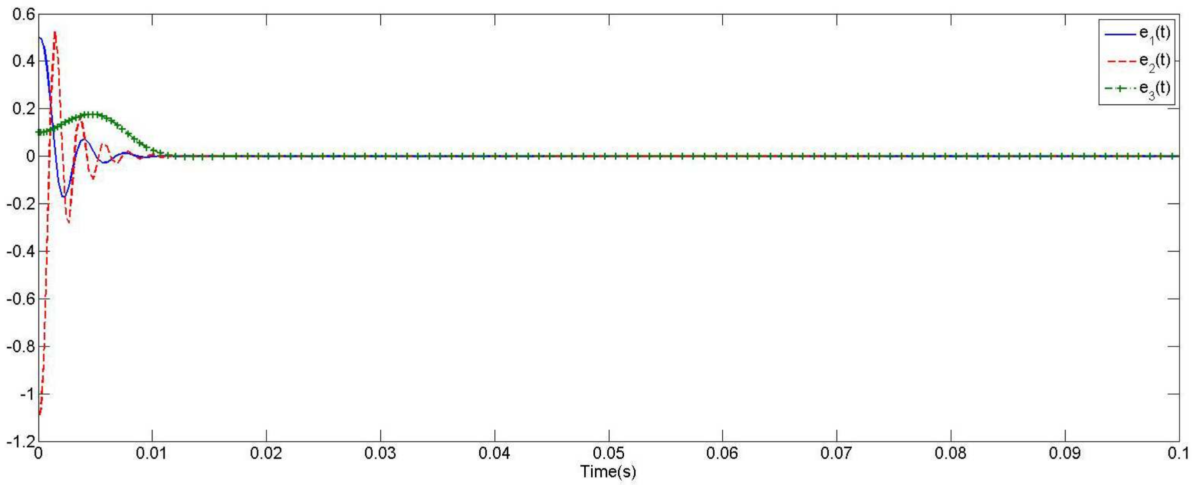

FIGURE 4. The controlled state trajectories $e_i(t)$ $(i = 1, 2, 3)$ of the error system

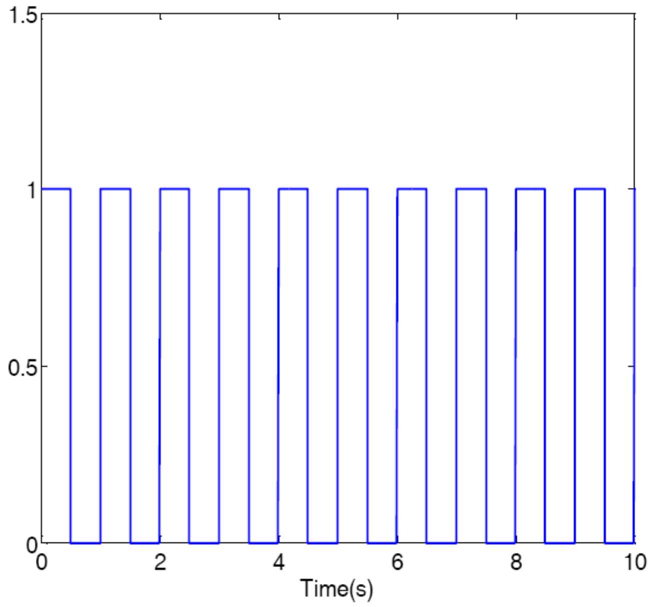

FIGURE 5. The information signal $S(t)$

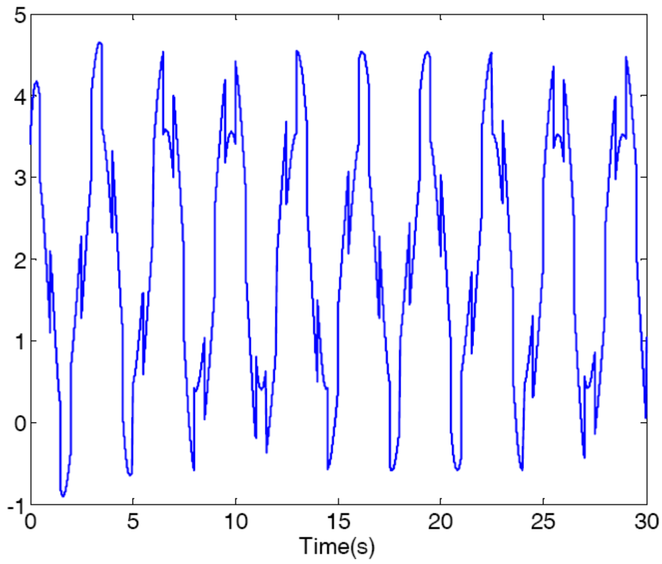

FIGURE 6. The transmitted signal $\chi(t)$

added to the variable x_2. Simulation results are presented in Figures 6-8. The transmitted signal is shown in Figure 6; apparently, no effect of the embedded modulating information signal can be depicted. Figure 7 displays the recovered signal $\tilde{S}(t)$, and one can observe that the recovered signal coincides with the original information signal with good accuracy. While the error between the original information signal and the recovered one is shown in Figure 8.

Example 2: $\beta_1 \neq \beta_2 \neq \beta_3$ and $x(0)$, $y(0)$ are selected as

$$\beta_1 = 4 + 0.2\sin(2t), \quad \beta_2 = 4 + 0.3\sin(3t), \quad \beta_3 = 4 + 0.1\sin(5t),$$
$$x_1(0) = 0.2, \quad x_2(0) = 0.6, \quad x_3(0) = 0.4,$$
$$y_1(0) = 0.6, \quad y_2(0) = 0.1, \quad y_3(0) = 0.9.$$

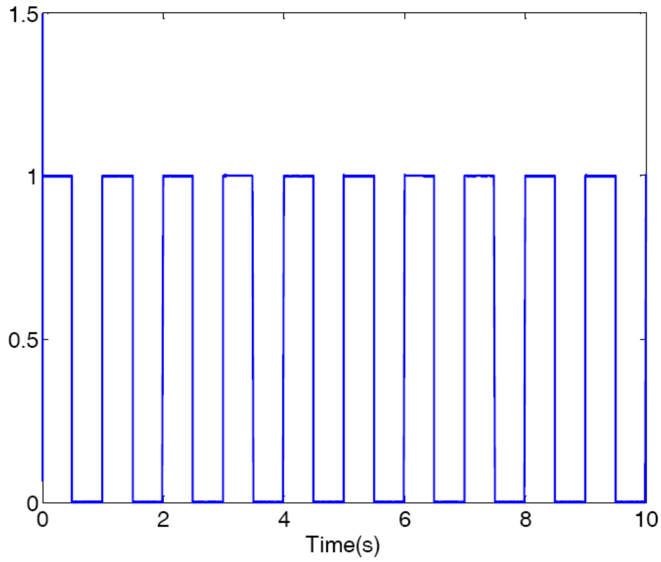

FIGURE 7. The recovered signal $\tilde{S}(t)$

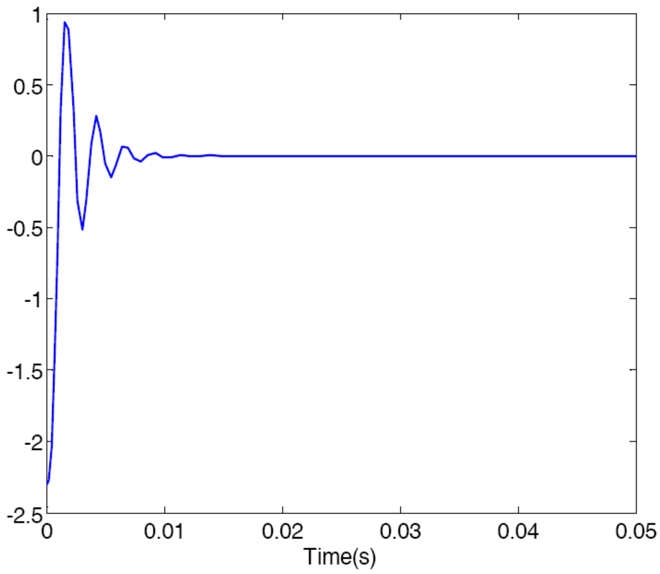

FIGURE 8. The error signal $\tilde{S}(t) - S(t)$

The following result can be obtained

$$P_1 = \begin{bmatrix} 2.5477 & 0.4984 & 0.5490 \\ 0.4984 & 1.5865 & 0.0437 \\ 0.5490 & 0.0437 & 0.9872 \end{bmatrix}, \quad P_2 = \begin{bmatrix} 0.8140 & -0.0997 & 0.0634 \\ -0.0997 & 0.5975 & 0.1765 \\ 0.0634 & 0.1765 & 0.3572 \end{bmatrix},$$

$$P_3 = \begin{bmatrix} 4.4223 & -0.7884 & -0.6557 \\ -0.7884 & 3.5620 & 1.0844 \\ -0.6557 & 1.0844 & 1.7510 \end{bmatrix}, \quad \begin{array}{lll} \varepsilon_1 = 8.0137, & \varepsilon_2 = 4.0025, & \varepsilon_3 = 8.0137, \\ \varepsilon_4 = 8.0137, & \varepsilon_5 = 4.0095, & \varepsilon_6 = 3.9958. \end{array}$$

The state trajectories of error system by using the proposed control scheme is shown in Figure 9, which implies that the mixed H_∞/passive function projective synchronization can be achieved for systems (8) and (12).

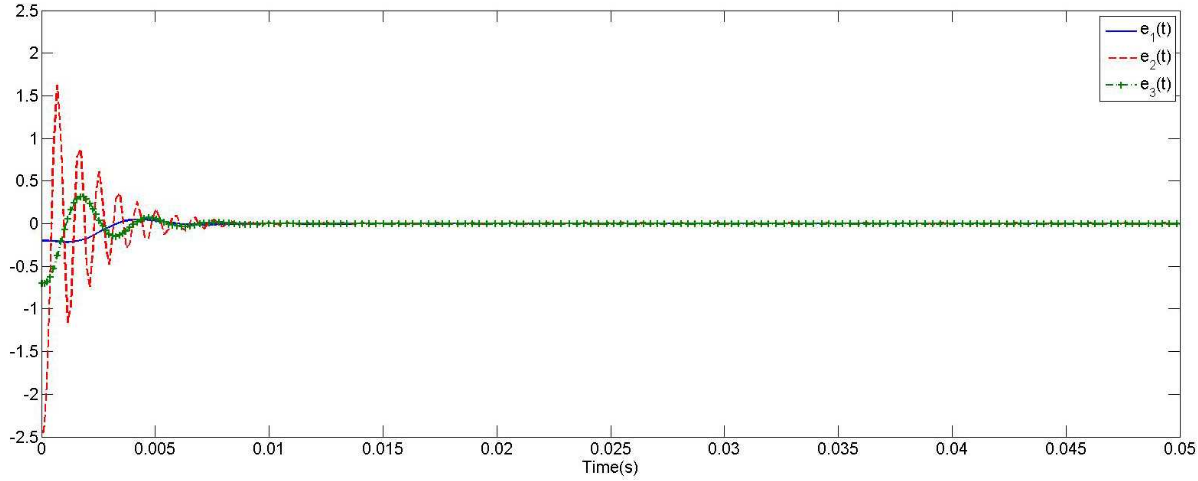

FIGURE 9. The controlled state trajectories $e_i(t)$ $(i = 1, 2, 3)$ of the error system

Remark 4.1. *In the Numerical Simulation part, two examples are given, and they are Example 1:* $\beta_1 = \beta_2 = \beta_3$*, and Example 2:* $\beta_1 \neq \beta_2 \neq \beta_3$*, respectively.*

In Example 1, firstly Case 1 is shown, which is a numerical example. The initial values in Case 1 are arbitrarily chosen to obey the rules that the considered drive and response systems under the chosen parameters show chaotic behaviors. Furthermore, under our proposed controller, the considered drive and response systems can be synchronized. From Figures 2-4, we can observe that the uncontrolled drive and response systems are chaotic and they cannot achieve synchronization. Figure 5 shows that the state trajectories of error system asymptotically converge to zero by using the proposed control scheme, which implies that the projective synchronization can be achieved for drive and response systems. Following Case 1 is Case 2, which is an application example in secure communications, and the aim is to show that our proposed method is valid in practical systems.

In Example 2, just β_i, $x_i(0)$, $y_i(0)$ $(i = 1, 2, 3)$ are different from the ones in Example 1, and the aim is to illustrate that our proposed method is valid for different β_i, $x_i(0)$, $y_i(0)$ $(i = 1, 2, 3)$.

5. **Conclusions.** In this paper, the mixed H_∞/passive projective synchronization problem for two time-delayed fractional-order neural networks with uncertain parameters has been studied. In terms of active control and adaptive control theory, a hybrid controller has been proposed to solve such a problem. Meanwhile, based on Lyapunov stability theory, the sufficient conditions are obtained, which can ensure the required mixed H_∞/passive performance level of the considered synchronization error system. Finally, the effectiveness of the proposed control scheme has been illustrated in numerical simulations.

Acknowledgments. This work is partially supported by the National Natural Science Foundation of China (Nos. U1604146, 61203047), Science and Technology Research Project in Henan Province (Nos. 152102210273, 162102410024) and China Scholarship Council (No. 201408410277). The authors would like to sincerely thank Prof. Om P. Agrawal and Prof. R. Koc (Chair), Mechanical Engineering and Energy Processes, Southern Illinois University for hosting her during April 8, 2016 to April 7, 2017.

REFERENCES

[1] C. A. Monje, Y. Q. Chen, B. M. Vinagre et al., *Fractional-Order Systems and Controls: Fundamentals and Applications*, Springer Science & Business Media, 2010.

[2] X. Huang, Z. Zhao, Z. Wang et al., Chaos and hyperchaos in fractional-order cellular neural networks, *Neurocomputing*, vol.94, pp.13-21, 2012.

[3] J. Chen, Z. Zeng and P. Jiang, Global Mittag-Leffler stability and synchronization of memristor-based fractional-order neural networks, *Neural Networks*, vol.51, pp.1-8, 2014.

[4] X. Yang, C. Li, Q. Song et al., Mittag-Leffler stability analysis on variable-time impulsive fractional-order neural networks, *Neurocomputing*, vol.207, pp.276-286, 2016.

[5] H. Bao, J. H. Park and J. Cao, Synchronization of fractional-order complex-valued neural networks with time delay, *Neural Networks*, vol.81, pp.16-28, 2016.

[6] L. M. Pecora and T. L. Carroll, Synchronization in chaotic systems, *Phys. Rev. Lett.*, vol.64, pp.821-824, 1990.

[7] P. Bagheri and M. Shahrokhi, Neural network-based synchronization of uncertain chaotic systems with unknown states, *Neural Computing & Applications*, vol.27, no.4, pp.945-952, 2016.

[8] A. Mohammadzadeh and S. Ghaemi, Synchronization of chaotic systems and identification of nonlinear systems by using recurrent hierarchical type-2 fuzzy neural networks, *ISA Transactions*, vol.58, pp.318-329, 2015.

[9] L. Ding, Projective synchronization of fractional-order chaotic systems based on sliding mode control, *Acta Physica Sinica*, vol.58, no.6, pp.3747-3752, 2009.

[10] J. Bai, Y. Yu, S. Wang et al., Modified projective synchronization of uncertain fractional order hyperchaotic systems, *Communications in Nonlinear Science & Numerical Simulation*, vol.17, no.4, pp.1921-1928, 2012.

[11] P. Zhou and W. Zhu, Function projective synchronization for fractional-order chaotic systems, *Nonlinear Analysis: Real World Applications*, vol.12, no.2, pp.811-816, 2011.

[12] Y. H. Yang, J. Xiao and Z. Z. Ma, Modified function projective synchronization for a class of partially linear fractional order chaotic systems, *Acta Physica Sinica*, vol.62, no.18, pp.116-121, 2013.

[13] H. Bao and J. Cao, Projective synchronization of fractional-order memristor-based neural networks, *Neural Networks*, vol.63, pp.1-9, 2015.

[14] J. Yu, C. Hu, H. Jiang et al., Projective synchronization for fractional neural networks, *Neural Networks*, vol.49, pp.87-95, 2014.

[15] S. Kuntanapreeda, Adaptive control of fractional-order unified chaotic systems using a passivity-based control approach, *Nonlinear Dynamics*, vol.84, no.4, pp.2505-2515, 2016.

[16] X. Song, S. Xu and H. Shen, Robust H_∞ control for uncertain fuzzy systems with distributed delays via output feedback controllers, *Information Sciences*, vol.178, no.22, pp.4341-4356, 2008.

[17] S. Xu, T. Chen and J. Lam, Robust H_∞ filtering for uncertain Markovian jump systems with mode-dependent time delays, *IEEE Trans. Automatic Control*, vol.48, no.5, pp.900-907, 2003.

[18] J. Shen and J. Lam, State feedback H_∞ control of commensurate fractional-order systems, *International Journal of Systems Science*, vol.45, no.3, pp.363-372, 2014.

[19] J. Shen and J. Lam, H_∞ model reduction for positive fractional order systems, *Asian Journal of Control*, vol.16, no.2, pp.441-450, 2014.

[20] K. Mathiyalagan, J. H. Park, R. Sakthivel et al., Robust mixed H_∞ and passive filtering for networked Markov jump systems with impulses, *Signal Processing*, vol.101, pp.162-173, 2014.

[21] H. Shen, Z. G. Wu and J. H. Park, Reliable mixed passive and H_∞ filtering for semi-Markov jump systems with randomly occurring uncertainties and sensor failures, *International Journal of Robust and Nonlinear Control*, vol.25, no.17, pp.3231-3251, 2015.

[22] L. Su and H. Shen, Mixed H_∞/passive synchronization for complex dynamical networks with sampled-data control, *Applied Mathematics and Computation*, vol.259, pp.931-942, 2015.

[23] I. Podlubny, *Fractional Differential Equations*, Academic Press, San Diego, 1999.

[24] L. Xie, Output feedback H_∞ control of systems with parameter uncertainty, *International Journal of Control*, vol.63, no.4, pp.741-750, 1996.

[25] L. Wang, Y. Shen and G. Zhang, General decay synchronization stability for a class of delayed chaotic neural networks with discontinuous activations, *Neurocomputing*, vol.179, pp.169-175, 2016.

[26] I. Stamova, Global Mittag-Leffler stability and synchronization of impulsive fractional-order neural networks with time-varying delays, *Nonlinear Dynamics*, vol.77, no.4, pp.1251-1260, 2014.

[27] H. Bao, J. H. Park and J. Cao, Adaptive synchronization of fractional-order memristor-based neural networks with time delay, *Nonlinear Dynamics*, vol.82, no.3, pp.1343-1354, 2015.

[28] W. K. Wong, H. Li and S. Y. S. Leung, Robust synchronization of fractional-order complex dynamical networks with parametric uncertainties, *Communications in Nonlinear Science and Numerical Simulation*, vol.17, no.12, pp.4877-4890, 2012.

[29] M. Gai, S. Cui, S. Liang et al., Frequency distributed model of Caputo derivatives and robust stability of a class of multi-variable fractional-order neural networks with uncertainties, *Neurocomputing*, vol.202, pp.91-97, 2016.

[30] X. Wu, H. Wang and H. Lu, Modified generalized projective synchronization of a new fractional-order hyperchaotic system and its application to secure communication, *Nonlinear Analysis: Real World Applications*, vol.13, no.3, pp.1441-1450, 2012.